

# Nonlocal Phonon Heat Transport Seen in Pulses

Philip B. Allen\* and Nhat A. Nghiem

*Department of Physics and Astronomy, Stony Brook University, Stony Brook, NY 11794-3800, USA*

(Dated: June 8, 2022)

The ballistic to diffusive crossover, that occurs when quasiparticles transport heat or charge, is important in small systems. Propagation of energy from an initial localized pulse provides a useful picture of the process. This paper looks at the simplest example, vibrational pulses on a one-dimensional harmonic chain of atoms. Pure ballistic propagation occurs in ordered chains, and a crossover toward diffusive propagation can be seen in disordered chains. A full analysis is inhibited by non-perturbative effects, especially Anderson localization. A partial analysis using Boltzmann theory is given.

## I. INTRODUCTION

In nonmagnetic insulators, phonons are the carriers of heat. Phonons have diverse mean free paths  $\ell_Q$ , diverging at small  $Q$ . The standard (local) Fourier law  $\vec{J} = -\kappa \vec{\nabla} T$  is not obeyed at locations (*e.g.* near boundaries) where local temperature  $T(\vec{r})$  varies on a length scale less than mean free paths of relevant phonons. Issues related to this (often called the “ballistic to diffusive crossover”) are important in nanoscale devices. There aren’t yet unifying theories, or prototype examples with detailed mathematical analysis. Numerical study of pulse propagation<sup>1</sup> provides simple insights but has not been used often. This paper looks at pulses on a one-dimensional harmonic chain, the simplest possible example<sup>2</sup>, and gives a partial analysis.

A generalized Fourier law, with a nonlocal conductivity  $\kappa(\vec{r}, \vec{r}'; t, t')$  relating current at  $\vec{r}, t$  to temperature gradient at other places and earlier times  $\vec{r}', t'$ , does not fully describe the problem. Hua and Lindsay<sup>3</sup> have recently shown that, in Boltzmann theory with external driving, there is an extra term,

$$\vec{J}(\vec{r}, t) = - \int d\vec{r}' \int_{-\infty}^t dt' \kappa(\vec{r} - \vec{r}', t - t') \vec{\nabla} T(\vec{r}', t') + \vec{B}(\vec{r}, t) \quad (1)$$

This equation applies when the medium is spatially homogeneous, but driven by a space and time-dependent external power insertion  $P_Q(\vec{r}, t)$ . The extra term  $\vec{B}$  varies with the  $Q$ -dependence of the inserted power. A similar term was found by Guyer and Krumhansl<sup>4</sup>. It is disappointing that a unique non-local response function ( $\kappa(\vec{k}, \omega)$  in reciprocal space) is insufficient and must be supplemented by a non-unique term  $\vec{B}$ .

Allen and Perebeinos<sup>5</sup> introduced a related but simpler response function,

$$\Delta T(\vec{r}, t) = \int d\vec{r}' \int_{-\infty}^t dt' \Theta(\vec{r} - \vec{r}', t - t') P(\vec{r}', t') + C(\vec{r}, t). \quad (2)$$

Here  $P$  is the mode average  $\sum_Q (C_Q/C) P_Q$ , with the specific heat  $C(T_0) = \sum_Q C_Q(T_0)$ . This connects the temperature rise  $\Delta T = T(\vec{r}, t) - T_0$  to the power inserted at

other places and earlier times  $(\vec{r}', t')$ . Similar to  $B(\vec{r}, t)$  in Eq. 1, the extra term  $C(\vec{r}, t)$  was not noticed until recently<sup>6</sup>. The version in ref. 5 did not take into account that the mathematical pulse form  $P$  could vary strongly with vibrational mode  $Q$ . For power insertion  $P(\vec{r}, t)$  independent of mode  $Q$ , the extra terms  $B(\vec{r}, t)$  and  $C(\vec{r}, t)$  vanish in Eqs. 1 and 2.

The name for the response function  $\Theta$  was originally “thermal susceptibility”, indicating a similarity to the electrical susceptibility relating charge to potential in a metal. However, the term “thermal susceptibility” is used with different meanings<sup>7,8</sup>, so a less confusing name, “thermal distributor”, is now used<sup>6</sup>. Focusing on the scalar response  $\Delta T$  to the scalar perturbation  $P$  has advantages; it is closer to the targets of nanoscale measurement<sup>9</sup> than the relation of the vector  $\vec{J}$  to the vector  $\vec{\nabla} T$ . Pulses are a good way to investigate this response. When  $P$  describes a pulse, it has  $(\vec{r}, t)$ -dependence that, in the continuum limit, is  $\sim \delta(\vec{r})\delta(t)$ . The temperature response  $\Delta T(\vec{k}, \omega)$  thus contains a picture of the response function  $\Theta(\vec{k}, \omega)$ . The two response functions are related by

$$\vec{k} \cdot \kappa(\vec{k}, \omega) \cdot \vec{k} - i\omega C = \frac{1}{\Theta(\vec{k}, \omega)}. \quad (3)$$

## II. ONE-DIMENSIONAL PULSES

The linear chain has  $N$  identical atoms of mass  $M$ , periodic boundary conditions, and nearest neighbor harmonic couplings with spring constant  $K$ ,

$$\mathcal{H} = \sum_{\ell} \left[ \frac{P_{\ell}^2}{2M} + \frac{1}{2} K(u_{\ell} - u_{\ell+1})^2 \right]. \quad (4)$$

The atoms have displacements  $u_{\ell}$  around average positions  $x = \ell a$ . The normal modes are labeled by wavevector  $Q$ . The general solution of Newton’s equations of motion is

$$u_{\ell}(t) = \sqrt{\frac{1}{N}} \sum_Q A_Q \cos(Q\ell a - \omega_Q t + \phi_Q), \quad (5)$$

There are  $2N$  free parameters (amplitude  $A_Q \geq 0$  and phase  $\phi_Q$  for each normal mode  $Q$ .) Their frequencies

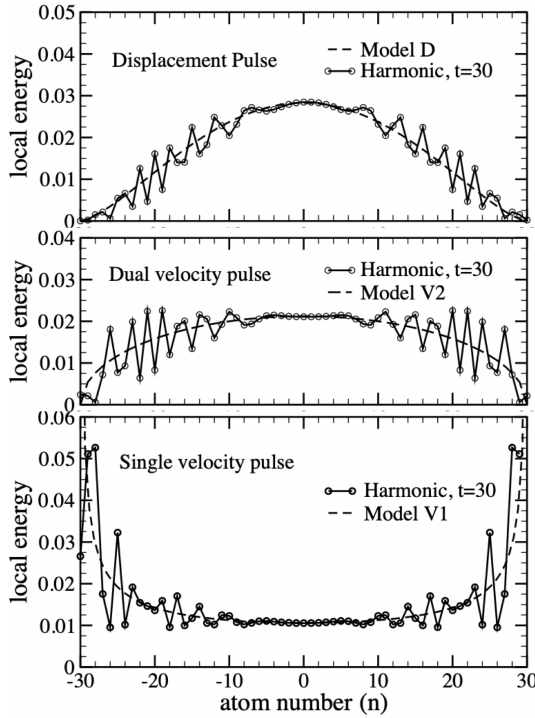


FIG. 1. Circles connected by solid lines are the computed local energy  $E_a(\ell)$  at  $t = 30$  for three types of pulses (see Eq. 6 and Table I). All three pulses evolve from energy inserted at  $t = 0$  and  $x \sim 0$  into a harmonic chain. The D and V2 pulses are initiated on atoms 0 and 1, but their positions on the horizontal axis are shifted by  $-1/2$  to make them symmetric around  $x = 0$ . The dashed curves are models derived from a continuum picture, such as Boltzmann theory, and given in Eqs. 13, 14, 15.

are  $\omega_Q = \omega_{\max} |\sin(Qa/2)|$  and group velocities are  $v_Q = v_{\max} \cos(Qa/2) \text{sign}(Q)$ . The maximum frequency and velocity are  $\omega_{\max} = 2\sqrt{K/M}$  and  $v_{\max} = a\sqrt{K/M}$ . Dimensionless units  $K = M = a = 1$  are used. Fig 1 shows three different pulses (labeled D, V2, and V1) after propagating for  $t = 30$  (the unit of time is  $2/\omega_{\max} = 1$ ).

The local energy  $E(\ell, t)$  at atom  $\ell$ , plotted in Fig. 1, is defined as

$$E_a(\ell) = \frac{P_\ell^2}{2M} + \frac{K}{4} [(u_{\ell-1} - u_\ell)^2 + (u_\ell - u_{\ell+1})^2]. \quad (6)$$

Each atom is assigned its own kinetic energy, and half of the potential energy of the springs to its left and right. This is the common definition, but it is not unique. Two other (randomly chosen but sensible) choices, for distributing potential energy to different sites, are

$$E_b(\ell) = \frac{P_\ell^2}{2M} + \frac{K}{2} [(2u_\ell^2 - u_\ell(u_{\ell-1} + u_{\ell+1}))], \quad (7)$$

$$E_c(\ell) = \frac{P_\ell^2}{2M} \text{ and } E_c(\ell + 1/2) = \frac{V}{2}(u_\ell - u_{\ell+1})^2. \quad (8)$$

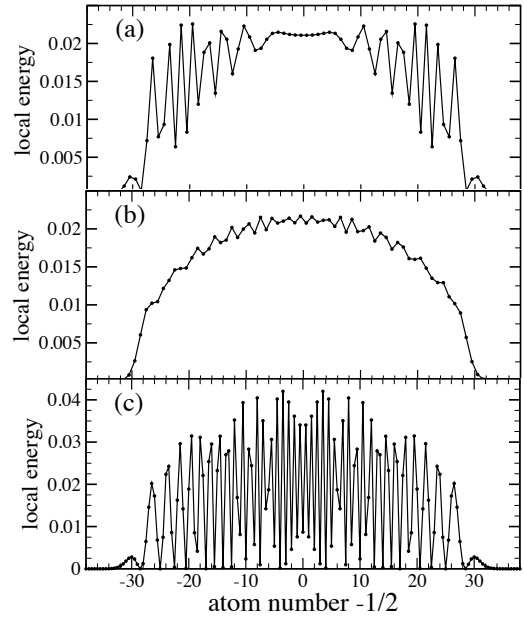


FIG. 2. The harmonic V2 pulse at  $T=0$  and time  $t=30$ , using three ways (Eqs. 6-8) of assigning potential energy to a local site energy,  $E(\ell)$ . In (a) and (b), the total energy is  $E = \sum_\ell E(\ell)$ . The area under the curves is  $E$ , chosen to be 1. In (c), however, the energy has an extra part  $\sum_\ell E(\ell+1/2)$ . The values in the graph have been arbitrarily doubled so that the total energy, also 1, is the area under the graph. These graphs demonstrate that the “continuum picture” of energy density, shown in Fig. 1, is probably less of an “approximation” than a local picture like these.

The conventional version  $E_a$  will be used in this paper, but it is interesting to see how it compares with versions  $E_b$  and  $E_c$ . The large oscillations seen in version (c) are surprising, and the smoothness seen in version (b) is even more surprising. shows that a continuum definition is probably more physical than the local version. Ambiguity also exists in quantum treatments. Marcolongo *et al.*<sup>10</sup> and Ercole *et al.*<sup>11</sup> have shown how this ambiguity does not affect the computation of bulk transport.

The definitions of the three types of pulses of Fig. 1 are given in Table I. The “V1” (or “velocity”) pulse has only the central atom given a velocity  $v_0$  at  $t = 0$ . The “V2” (or “dual velocity”) pulse has two central atoms given equal and opposite velocities. The “D” (or “displacement”) pulse has two central atoms given equal and opposite displacements at  $t = 0$ .

Figure 1 shows  $E_a(\ell, t)$  at  $t = 30$  for the three types of pulses, inserted at  $t = 0$  into zero-temperature (*i.e.* stationary) chains. Figure 3 shows the same pulse forms, at  $t = 20$ , inserted into chains with a pre-existing thermal distribution of velocities and displacements. In  $T > 0$  cases, the initial pulse amplitudes ( $\Delta u_{0,1}$  or  $\Delta v_{0,1}$ ) are scaled from those in table I to make the total extra energy  $\sum_\ell \Delta E_a(\ell)$  of the pulse equal to 1. The pulse profiles in Figs. 1 and 3 were computed in two different ways: (1) by numerical integration of Newton’s laws, and (2),

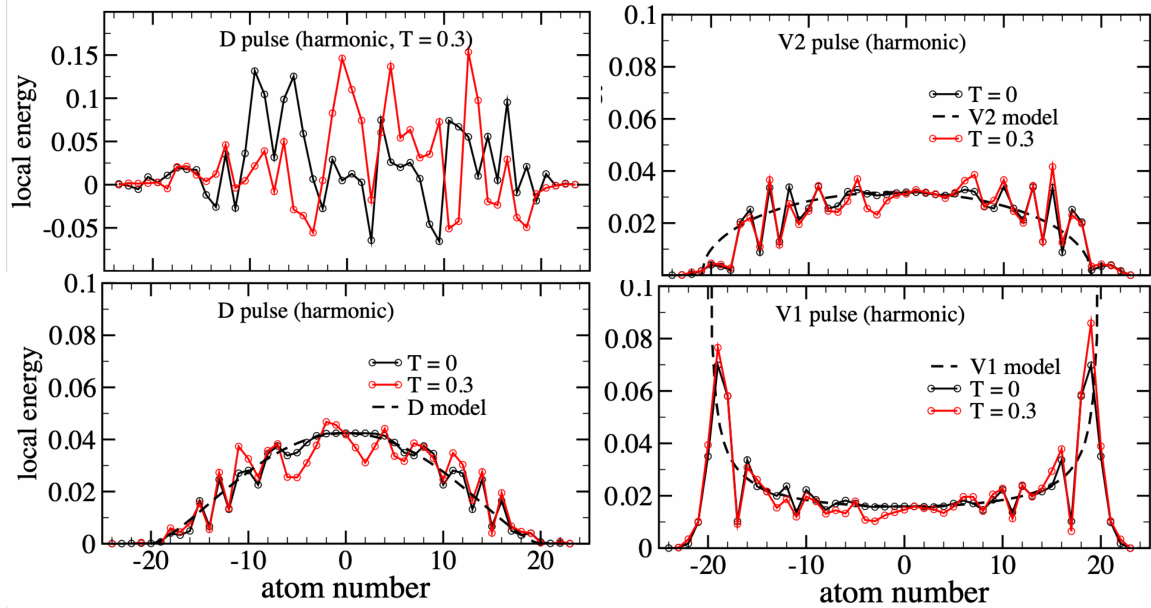


FIG. 3. Pulses of total energy  $\sum_\ell \Delta E_a(\ell) = 1$  at  $t = 20$ , inserted at  $t = 0$  to chains whose random positions and velocities at  $t = 0^-$  correspond to thermalization at temperature  $T = 0.3$  ( $E_{\text{tot}} = 0.3N$ ). The local energies  $\Delta E_a(\ell)$  shown in the graphs are the differences between  $E_a(\ell, t = 20)$  with and without pulse insertion. The first graph shows D pulses inserted with two typical initial conditions. The other graphs show, in red, the results averaged over 1000-member ensembles with random thermal initial conditions. The black results repeat the zero-temperature pulses shown in Fig. 1. The finite  $T$  pulse shapes, after ensemble averaging, are converging towards the zero-temperature pulse shapes.

name	$\Delta u_0$	$\Delta u_1$	$\Delta v_0$	$\Delta v_1$
V1	0	0	$\sqrt{2}$	0
V2	0	0	-1	1
D	$-1/\sqrt{3}$	$1/\sqrt{3}$	0	0

TABLE I. Properties of pulses. The shift  $\Delta u$  of initial displacement, or  $\Delta v$  of initial velocity, is scaled so that the new coordinates  $(u_0 + \Delta u_0, u_1 + \Delta u_1, v_0 + \Delta v_0, v_1 + \Delta v_1)$  have a total pulse energy equal to 1. The values in the table are the ones that work at  $T = 0$ , where  $u_0 = 0$ , etc.

by finding the coefficients  $A_Q$  and  $\phi_Q$  in Eq. 5. These coefficients are independent of time, and can be found if the positions  $u_\ell$  and velocities  $v_\ell = du_\ell/dt$  are known at any chosen time:

$$A_Q e^{i(\phi_Q - \omega_Q t)} = \sqrt{\frac{1}{N}} \sum_\ell \left[ u_\ell(t) + i \frac{v_\ell(t)}{\omega_Q} \right] e^{-iQ\ell a}. \quad (9)$$

For the  $T = 0$  case, values of  $A_Q$  and  $\phi_Q$  are given in table II. They are derived from the  $t = 0$  positions and velocities shown in table I at  $t = 0$ .

The chains are harmonic, so the pulses propagate ballistically. The leading edges propagate at the velocity of sound,  $\pm v_{\text{max}}$ . The left or right parts have root mean square (rms) displacements  $\bar{x}$  defined as

$$\bar{x}(t) \equiv \left[ \frac{\sum_\ell (\ell a)^2 \Delta E(\ell, t)}{\sum_\ell \Delta E(\ell, t)} \right]^{1/2}. \quad (10)$$

name	Amplitude $A_Q$ from Eq. 9	phase $\phi_Q$	modal energy $E(Q)$
V1	$\frac{\Delta v_0}{\sqrt{N} \omega_Q}$	$\frac{\pi}{2}$	$\frac{E_0}{N}$
V2	$\frac{2\Delta v_0}{\sqrt{N} \omega_Q} \sin\left(\frac{Qa}{2}\right)$	$\pi - \frac{Qa}{2}$	$\frac{2E_0}{N} \sin^2\left(\frac{Qa}{2}\right)$
D	$\frac{2\Delta u_0}{\sqrt{N}} \sin\left(\frac{Qa}{2}\right)$	$-\frac{\pi}{2} - \frac{Qa}{2}$	$\frac{8E_0}{3N} \sin^4\left(\frac{Qa}{2}\right)$

TABLE II. More properties of pulses: the distribution among normal modes  $Q$  of the phonon amplitude  $A_Q$ , phase  $\phi_Q$ , and energy, for the pulses of table I inserted at  $T = 0$ .

The rms displacements propagate at slower speeds. Values  $v_{\text{rms}} = d\bar{x}/dt \sim \pm v_{\text{max}}/\sqrt{n}$ , with  $n = 2, 4, 6$  for the V1, V2, and D pulses, respectively, follow from the continuum description described next.

The energy content of each normal mode is

$$E(Q) = \frac{1}{2} M \omega_Q^2 A_Q^2. \quad (11)$$

Using values of  $A_Q$  from Table II, the mode energies are also shown in Table II. The continuum version is ignorant of specific atomic coordinates, and finds an alternate definition of the local energy density  $E(x, t)$ . An appropriate continuum hypothesis for a pulse originating at  $(x, t) = (0, 0)$  is

$$E(x, t) = \sum_Q E(Q) \delta(x - v_Q t). \quad (12)$$

After integrating over  $Q$ , the results for the three pulses are

$$E_{V1}(x, t) = \frac{E_0}{\pi v_M t} \left( 1 - \left( \frac{x}{v_M t} \right)^2 \right)^{-1/2} \theta(v_M t - |x|), \quad (13)$$

$$E_{V2}(x, t) = \frac{2E_0}{\pi v_M t} \left( 1 - \left( \frac{x}{v_M t} \right)^2 \right)^{1/2} \theta(v_M t - |x|), \quad (14)$$

$$E_D(x, t) = \frac{8E_0}{3\pi v_M t} \left( 1 - \left( \frac{x}{v_M t} \right)^2 \right)^{3/2} \theta(v_M t - |x|). \quad (15)$$

The total energy  $\int dx E(x, t)$  is  $E_0$  in all three cases. These formulas are shown as dashed lines in Figs. 1 and 3. The continuum model agrees well with an average of nearby values of the local atomic energy  $E(\ell)$  for all of the three versions  $E_\alpha(\ell)$ . The rms centers of energy of the propagating pulses are then

$$\bar{x}_{\text{continuum}}(t) \equiv \left[ \frac{\int dx x^2 E(x, t)}{\int dx E(x, t)} \right]^{1/2}. \quad (16)$$

This is where the result  $d\bar{x}/dt \sim \pm v_{\text{max}}/\sqrt{n}$  (with  $n = 2, 4, 6$ ) came from.

It had been our original guess that when the pulse propagates in a thermal background, the fine structure in  $E(\ell)$  would disappear and the result would resemble the continuum version  $E(x)$ . The computation in Fig. 3 shows that this guess was wrong. The fine structure remains. A proof that this should happen is given in the appendix.

### III. BOLTZMANN EQUATION

The formulas given in Eqs. 13, 14, 15 came from a sensible hypothesis, Eq. 12. Re-deriving this from Boltzmann theory gives useful insight. The Peierls Boltzmann equation uses quantum wave/particle duality to deal with phonons as a gas of particles, which can be treated classically or quantum mechanically.

$$\frac{\partial N_Q}{\partial t} = -v_Q \frac{\partial N_Q}{\partial x} + \left( \frac{\partial N_Q}{\partial t} \right)_{\text{coll}} + \left( \frac{\partial N_Q}{\partial t} \right)_{\text{ext}}. \quad (17)$$

The function  $N_Q(x, t)$  is the occupancy per unit length of phonon mode  $Q$  at  $(x, t)$ . The spatial sum  $\int dx N_Q(x, t) = N_Q(t)$  is the mode occupancy. Even though our treatment of the linear chain is classical, it is sensible to use the quantum version, with an equilibrium distribution  $N_Q \rightarrow n_Q(T_0) = [\exp(\hbar\omega_Q/k_B T_0) - 1]^{-1}$  rather than the classical limit  $n_Q = k_B T_0 / \hbar\omega_Q$ .

The scattering (or collision) term  $(\partial N_Q/\partial t)_{\text{coll}}$ , is dropped, because the perfect harmonic linear chain has

phonon modes  $Q$  that never decay. The chains are driven by an external manipulation that changes the Newtonian state  $\{u_\ell, v_\ell\}$  to  $\{u_\ell + \Delta u_\ell, v_\ell + \Delta v_\ell\}$ . This alters phonon amplitudes and phases to give the starting pulse shape. This needs to be accomplished by the term  $(\partial N_Q/\partial t)_{\text{ext}}$  in the Boltzmann equation. External driving  $(\partial N_Q/\partial t)_{\text{ext}}$  has only recently appeared in phonon Boltzmann theory<sup>12-15</sup>, and its form and significance are not yet fully understood. Boltzmann theory does not deal directly with amplitudes  $A_Q$ . These are indirectly included via the mode energy  $MA_Q^2\omega_Q^2/2 \sim \hbar\omega_Q N_Q$ . Boltzmann theory does not deal at all with phases  $\phi_Q$ . The external term  $(\partial N_Q/\partial t)_{\text{ext}}$  drives the distribution function  $N_Q$  away from equilibrium  $n_Q(T_0)$  to  $n_Q(T_0) + \Phi_Q(x, t)$ . Linearizing in  $\Phi_Q$ , the driving term has the form

$$\left( \frac{\partial N_Q}{\partial t} \right)_{\text{ext}} = R_Q \delta(x) \delta(t). \quad (18)$$

$$R_Q = \frac{\Delta E_Q^{\text{pulse}}}{\hbar\omega_Q}, \quad (19)$$

the pulse energy inserted into mode  $Q$ , divided by the quantum of energy in that mode. The total pulse energy given to the system is clearly correct:

$$E_{\text{pulse}}^{\text{Boltzmann}} = \int dx \int dt \sum_Q \hbar\omega_Q (\partial N_Q / \partial t)_{\text{ext}} = \sum_Q \hbar\omega_Q R_Q = \sum_Q \Delta E_Q^{\text{pulse}}. \quad (20)$$

Because of linearity and periodic boundary conditions, it is convenient to Fourier transform to  $N_Q(k, \omega)$ ,

$$N_Q(k, \omega) = \frac{1}{L} \int_{-L/2}^{L/2} dx \int_{-\infty}^{\infty} dt N_Q(x, t) e^{-i(kx - \omega t)}. \quad (21)$$

The collisionless Boltzmann equation is then easily solved in Fourier space, and transformed back,

$$\begin{aligned} \Delta N_Q(x, t) &= \frac{L}{2\pi} \int dk \int \frac{d\omega}{2\pi} \frac{R_Q}{-i(\omega + i\eta - kv_Q)} e^{i(kx - \omega t)} \\ &= R_Q \delta(x - v_Q t) \end{aligned} \quad (22)$$

The  $\Delta$  here allows the finite  $T$  distribution to be  $n_Q(T_0) + \Delta N_Q$ , and is not needed at  $T = 0$  where  $n_Q = 0$ . The local energy density is

$$\bar{E}_{\text{pulse}}(x, t) = \sum_Q \hbar\omega_Q \Delta N_Q(x, t) = \sum_Q \Delta E_Q^{\text{pulse}} \delta(x - v_Q t). \quad (23)$$

This agrees exactly with Eq. 12. These results improve confidence in the new insertion term added to the Peierls Boltzmann equation. We also learn that, in the continuum description, the pulse shapes (Eqs. 13-15) are independent of  $T$ , because the temperature  $T_0$  in the Boltzmann treatment did not have to be specified. The less obvious result, that pulse shapes in the atomistic version are also independent of  $T$ , is shown in the Appendix.

#### IV. MASS DISORDER

Disorder adds interesting complications to 1-d harmonic crystals. Disorder causes Anderson localization of all single-particle electron eigenstates, in disordered metals of dimension 2 or less<sup>16</sup>. Localization of phonons is similar<sup>17-19</sup>. All phonon normal modes on a 1-d disordered chain are localized if the chain is long enough. Quasiparticle theory and perturbation theory do not work at long distances in  $d = 1$ , but at intermediate distances, if disorder is not too great, are likely to be useful. Reference 2 gives the example of a wave packet propagating on a weakly mass-disordered chain. Ballistic propagation is seen at short distances and times, diffusive propagation at intermediate ones, and Anderson localization at long distances and times.

A problem is immediately obvious when using the Fermi golden rule for phonon decay rates,  $1/\tau_Q = (2\pi/\hbar) \sum_{Q'} |V_{QQ'}|^2 \delta(\hbar\omega_Q - \hbar\omega_{Q'})$ . The interaction  $V_{QQ'}$  can contain either mass or spring-constant disorder. Second order perturbation theory can never drive the phonon gas to redistribute energies of normal modes to a thermal distribution, since scattering conserves the number of phonons with energy  $\hbar\omega_Q$ . In higher order, pairs of phonons of energy  $\omega_1 + \omega_2$  can scatter to other pairs  $\omega_3 + \omega_4$  with the same total energy, and thus evolve toward equilibrium. But at long times, Anderson localization, a non-perturbative effect, prohibits use of perturbative treatments. Boltzmann theory usually uses only second-order scattering, so seems hard to apply to the ballistic to diffusive crossover, and is not applicable to the diffusive to localized crossover.

We now use mass defects to see how they weaken ballistic propagation. We randomly choose 10% of the atoms, and increase their masses from  $M = 1$  to  $M = 1.5$ . Results at various times for a D pulse are shown in Fig. 4. The lattice is still harmonic, but the Hamiltonian is no longer diagonal in the plane-wave basis, Eq. 5. Before ensemble averaging, the pulse shape varies depending on the locations of the mass defects relative to the point of pulse insertion. The D-pulse shapes of Fig. 4 have been averaged over 100 different random placements of the altered masses.

The pulse shape at  $t = 10\sqrt{M/K}$  is not much altered from pure ballistic behavior. The pulse has propagated only a distance of  $\pm 10$  atoms, and encountered typically only two impurities. As time proceeds, there is increasing deviation from the ballistic line shape predicted in Eq. 15, and shown in the red curves. By  $t=40$ , the fraction of the energy in the leading ballistic edge is noticeably diminished, and the fraction in the interior  $\pm 10$  atoms has failed to diminish the way ballistic propagation does. Diffusion is increasingly taking over. The disorder is relatively weak, so the Anderson localization lengths  $\xi_Q$  are probably mostly longer than the propagation distance of  $\pm 40$  atoms studied here.

Even though a Boltzmann analysis is both questionable and more difficult than we wish to attempt, one

might still wonder whether Boltzmann theory in relaxation time approximation (RTA) could be used. If the term  $(\partial N_Q/\partial t)_{\text{coll,RTA}} = -\Phi_Q/\tau_Q$  is added to Eq. 17, the solution is the same as Eq. 22 except that the infinitesimal  $\eta$  is replaced by  $1/\tau_Q$ . The result is clearly inappropriate: Eq. 23 acquires a factor  $\exp(-t/\tau_Q)$ . This may offer a sensible description of the decay of ballistic propagation, but offers no hint of the desired diffusion. It just destroys the ballistic energy without replacing it. It is surprising how inapplicable RTA is to this  $(x, t)$ -dependent case, considering how successful it is in bulk time-independent quasiparticle conductivity.

Here is a sensible phenomenological guess for how the ballistic/diffusive crossover might happen.

$$N_Q^{\text{guess}}(x, t) = n(T_0) + \Delta N_Q^{\text{ball}}(x, t) + \Delta N_Q^{\text{diff}}(x, t), \quad (24)$$

$$\Delta N_Q^{\text{ball}}(x, t) = \theta(t) R_Q e^{-t/\tau_Q} \delta(x - v_Q t), \quad (25)$$

$$\Delta N_Q^{\text{diff}}(x, t) = \theta(t) R_Q \left(1 - e^{-t/\tau_Q}\right) \frac{e^{-x^2/4D_Q t}}{\sqrt{4\pi D_Q t}}. \quad (26)$$

Equation 25 is the RTA solution. Equation 26 is a guess with no precise Boltzmann origin. The quantity  $D_Q \equiv v_Q^2 \tau_Q$  is the mode diffusivity. The sum of Eqs. 25 and 26 has been forced to conserve mode energy. The rate  $1/\tau_Q$  is the lifetime broadening of state  $Q$  caused by mass defects. To second order, the formula<sup>20,21</sup> is

$$\begin{aligned} \frac{1}{\tau_Q} &= \frac{\pi}{2\hbar} \frac{N_i}{N} \left( \frac{\Delta M}{M + \Delta M} \right)^2 (\hbar\omega_Q)^2 \mathcal{D}(\omega_Q) \\ &= \epsilon \frac{\omega_Q^2}{(\omega_M^2 - \omega_Q^2)^{1/2}}, \quad \text{where } \epsilon = \frac{N_i}{N} \left( \frac{\Delta M}{M + \Delta M} \right)^2, \end{aligned} \quad (27)$$

where the density of vibrational states of the ordered harmonic chain is

$$\mathcal{D}(\omega) = \frac{1}{\hbar N} \sum_Q \delta(\omega - \omega_Q) = \frac{2}{\pi\hbar} \frac{1}{(\omega_M^2 - \omega^2)^{1/2}}, \quad (28)$$

This hypothesis is tested in Fig. 5, with no adjustable parameters. The fit is not impressive, but is a sensible caricature of what is happening. The disagreement between hypothesis and numerical computation does not look like it could be caused by localization.

#### V. ACKNOWLEDGEMENTS

We are grateful to the Stony Brook Institute for Advanced Computational Science for use of their computer cluster.

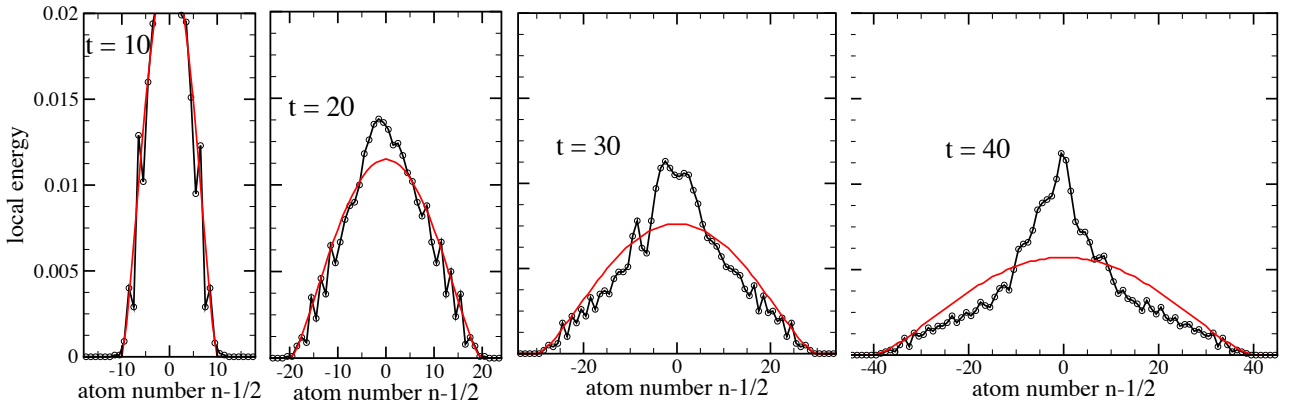


FIG. 4. Total energy profile  $E_a(\ell)$  of a **D**-pulse at  $T = 0$ , after spreading in the lattice with 10% of the masses increased by 1.5. The profiles are averaged over 100 random realizations of mass disorder. Time is in units  $\sqrt{M/K}$ . The red curves are the ballistic prediction of Eq. 15.

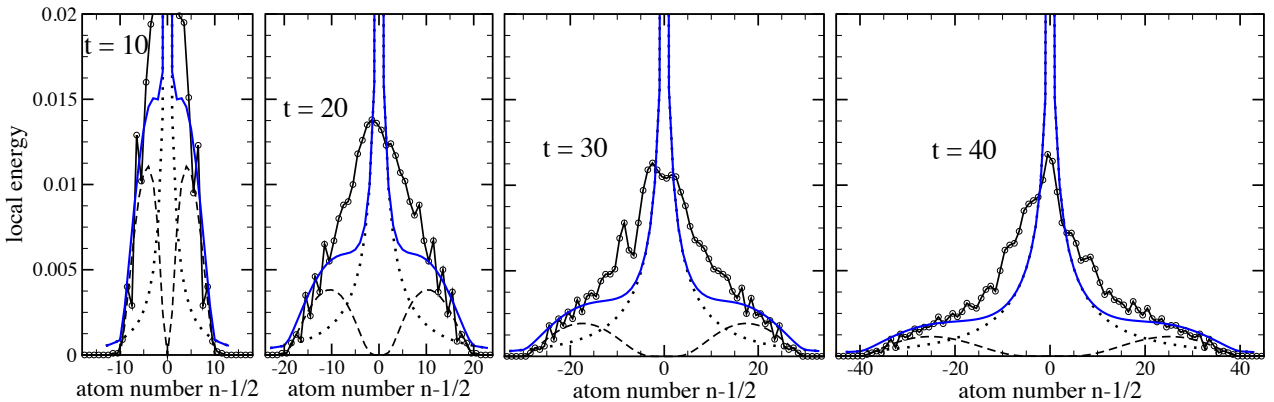


FIG. 5. The same total energy profile of a **D**-pulse at  $T = 0$ , shown in Fig. 4. The dashed curve is the decaying ballistic model, Eq. 25, and the dotted curve is the correspondingly growing diffusive model, Eq. 26. The blue curve is the sum of these two models.

## VI. APPENDIX: DETAILS

The most general harmonic linear chain is described by

$$\mathcal{H} = \frac{1}{2} \sum_{\ell} \dot{w}_{\ell}^2 + \frac{1}{2} \sum_{\ell} \Omega_{\ell\ell'} w_{\ell} w_{\ell'}, \quad (29)$$

where  $w_{\ell} = \sqrt{M_{\ell}} u_{\ell}$  and  $\Omega_{\ell\ell'} = K_{\ell,\ell'} / \sqrt{M_{\ell} M_{\ell'}}$ . The spring constant  $K_{\ell\ell'}$  is  $\partial^2 U_{\text{PE}} / \partial u_{\ell} \partial u_{\ell'}$ . Vibrational eigenstates  $|\mu\rangle$  are solutions of  $\hat{\Omega}|\mu\rangle = \omega_{\mu}^2 |\mu\rangle$ . The general solution of Newton's laws is described by  $N$  amplitudes  $A_{\mu}$  and phases  $\phi_{\mu}$ ,

$$w_{\ell}(t) = \frac{1}{\sqrt{N}} \sum_{\mu} A_{\mu} \mu_{\ell} \cos(\omega_{\mu} t - \phi_{\mu}), \text{ where } \mu_{\ell} = \langle \ell | \mu \rangle. \quad (30)$$

The normal mode coordinates  $\mu_{\ell} = \langle \ell | \mu \rangle$  are defined to be real numbers. For ordered chains of atoms, the simpler convention is to use complex numbers  $\langle \ell | Q \rangle =$

$\exp(iQ\ell a) / \sqrt{N}$ , but real numbers (cosines and sines) also work.

The normal modes are orthonormal,

$$\langle \mu | \mu' \rangle = \sum_{\ell} \langle \mu | \ell \rangle \langle \ell | \mu' \rangle = \frac{1}{N} \sum_{\ell} \mu_{\ell} \mu'_{\ell} = \delta_{\mu\mu'}. \quad (31)$$

From this it is easy to show that

$$\begin{aligned} \text{KE} &= \frac{1}{2} \sum_{\mu} \omega_{\mu}^2 A_{\mu}^2 \sin^2(\omega_{\mu} t - \phi_{\mu}), \\ \text{PE} &= \frac{1}{2} \sum_{\mu} \omega_{\mu}^2 A_{\mu}^2 \cos^2(\omega_{\mu} t - \phi_{\mu}), \end{aligned} \quad (32)$$

and therefore the total energy is

$$E_{\text{tot}} = \sum_{\mu} E_{\mu}, \text{ where } E_{\mu} = \frac{1}{2} \omega_{\mu}^2 A_{\mu}^2. \quad (33)$$

This is the generalization to lattices (whether ordered or disordered), of Eq. 11 for ordered lattices. It is also easy

to derive the formula

$$A_\mu e^{i(\phi_\mu - \omega_\mu t)} = \frac{1}{\sqrt{N}} \sum_\ell \sqrt{M_\ell} \left( u_\ell(t) + i \frac{v_\ell(t)}{\omega_\mu} \right) \mu_\ell. \quad (34)$$

This is the generalization of Eq. 9. From this formula, one can extract the amplitude  $A_\mu$  and phase  $\phi_\mu$  of any normal mode  $\mu$  if the positions  $u_\ell$  and velocities  $v_\ell$  are known at any particular time  $t$ . For example, consider a V1 pulse inserted at zero temperature. Using Eq. 34, the modal energy is

$$E_\mu^{\text{V1}, T=0} = \frac{1}{2} \omega_\mu^2 A_\mu^2 = \frac{M_0}{2N} \Delta v_0^2 \mu_0^2 = E_{\text{pulse}}^{\text{V1}} \frac{\langle 0|\mu\rangle\langle\mu|0\rangle}{N}$$

$$E_{\text{pulse}}^{\text{V1}} = \sum_\mu E_\mu^{\text{V1}, T=0} = \frac{M_0 \Delta v_0^2}{2}. \quad (35)$$

From these results, we can make a tedious proof (for the V1 case) that when temperature is not zero, the ensemble average energy in each mode  $\mu$  continues to obey Eq. 35. This means that the ensemble average pulse shape is unaffected by temperature, for both ordered and disordered chains, agreeing with our simulation results in Fig. 3 for the ordered chain. For any particular member of the ensemble, the mode  $\mu$  has energy  $\frac{1}{2} \omega_\mu^2 A_\mu^2$  before pulse insertion, and  $\frac{1}{2} \omega_\mu^2 (A_\mu + \Delta A_\mu)^2$  after. Using Eq. 34, this can be written as

$$E_\mu^{\text{before}} = [f_\mu + ig_\mu v_0][f_\mu^* - ig_\mu v_0]$$

$$E_\mu^{\text{after}} = [f_\mu + ig_\mu (v_0 + \Delta v_0)][f_\mu^* - ig_\mu (v_0 + \Delta v_0)], \quad (36)$$

where

$$f_\mu = \sqrt{\frac{1}{2N}} \left[ \sum_\ell^{\neq 0} \sqrt{M_\ell} (\omega_\mu u_\ell + iv_\ell) \mu_\ell + \sqrt{M_0} \omega_\mu u_0 \mu_0 \right] \quad (37)$$

$$\text{and } g_\mu = \sqrt{\frac{M_0}{2N}} \mu_0. \quad (38)$$

The point of Eq. 36 is to separate the coordinate  $v_0$  or  $v_0 + \Delta v_0$  from the remaining coordinates  $u_\ell, v_\ell$  which are collected in  $f_\mu$ . This enables ensemble averages to be done using the fact that  $\langle f_\mu v_0 \rangle_T = \langle f_\mu \rangle_T \langle v_0 \rangle_T = 0$  and  $\langle f_\mu \Delta v_0 \rangle_T = \langle f_\mu \rangle_T \langle \Delta v_0 \rangle_T = 0$ . The null values follow from the fact that  $\langle f_\mu \rangle_T = 0$ . Note that  $\langle \Delta v_0 \rangle_T \neq 0$ ;  $\Delta v_0$  is chosen to make the V1 pulse have a fixed energy  $E_{\text{pulse}}$ , for every member of the ensemble. This requires

$$\frac{1}{2} M_0 [(v_0 + \Delta v_0)^2 - v_0^2] = E_{\text{pulse}}^{\text{V1}} \quad (39)$$

whether ensemble-averaged or not. This is the general version of the  $T = 0$  form in Eq. 35 which has  $v_0 = 0$ . From Eq. 36 we get

$$\Delta E_\mu^{\text{V1}} = g_\mu^2 [(v_0 + \Delta v_0)^2 - v_0^2] - i(f_\mu - f_\mu^*) g_\mu \Delta v_0. \quad (40)$$

The ensemble average is

$$\langle \Delta E_\mu^{\text{V1}} \rangle_T = g_\mu^2 \langle [(v_0 + \Delta v_0)^2 - v_0^2] \rangle_T. \quad (41)$$

Finally, using Eqs. 35, 38, and 39, we get

$$\langle \Delta E_\mu^{\text{V1}} \rangle_T = E_{\text{pulse}}^{\text{V1}} \frac{\mu_0^2}{N}, \text{ and } \sum_\mu \langle \Delta E_\mu^{\text{V1}} \rangle_T = E_{\text{pulse}}^{\text{V1}}. \quad (42)$$

This proof is sufficiently tedious that the corresponding proofs for V2 and D pulses have not been checked. The results of Fig. 3 indicate that probably all pulses on harmonic chains have shapes independent of  $T$  after ensemble averaging.

<sup>1</sup> philip.allen@stonybrook.edu

<sup>2</sup> Sha Liu, P. Hänggi, Nianbei Li, Jie Ren, and Baowen Li, “Anomalous heat diffusion,” *Phys. Rev. Lett.* **112**, 040601 (2014).

<sup>3</sup> P. B. Allen and J. Kelner, “Evolution of a vibrational wave packet on a disordered chain,” *Am. J. Phys.* **66**, 497–506 (1998).

<sup>4</sup> Chengyun Hua and Lucas Lindsay, “Space-time dependent thermal conductivity in nonlocal thermal transport,” *Phys. Rev. B* **102**, 104310 (2020).

<sup>5</sup> R. A. Guyer and J. A. Krumhansl, “Solution of the linearized phonon Boltzmann equation,” *Phys. Rev.* **148**, 766–778 (1966).

<sup>6</sup> P. B. Allen and V. Perebeinos, “Temperature in a Peierls-Boltzmann treatment of nonlocal phonon heat transport,” *Phys. Rev. B* **98**, 085427 (2018).

<sup>7</sup> P. B. Allen, “Phonon Boltzmann equation non-local in space and time: the partial failure of the generalized Fourier law,” ArXiv e-prints (2021), arXiv:2105.14413 [cond-mat.mes-hall].

<sup>8</sup> S. Volz, R. Carminati, and K. Joulain, “Thermal response of silicon crystal to pico-femtosecond heat pulse by molecular dynamics,” *Microscale Thermophysical Engineering* **8**, 155 – 167 (2004).

<sup>9</sup> M. Baiesi, U. Basu, and C. Maes, “Thermal response in driven diffusive systems,” *The European Physical Journal* **87**, 277:1–10 (2014).

<sup>10</sup> L. Dias Carlos and F. Palacio, *Thermometry at the Nanoscale* (Roy. Soc. Chem., Cambridge, 2016).

<sup>11</sup> A. Marcolongo, P. Umari, and S. Baroni, “Microscopic theory and quantum simulation of atomic heat transport,” *Nature Physics* **12**, 80 – 84 (2016).

<sup>11</sup> L. Ercole, A. Marcolongo, P. Umari, and S. Baroni, “Gauge invariance of thermal transport coefficients,” *J. Low Temp. Phys.* **185**, 79–86 (2016).

<sup>12</sup> Chengyun Hua and A. J. Minnich, “Analytical Green’s function of the multidimensional frequency-dependent phonon Boltzmann equation,” *Phys. Rev. B* **90**, 214306 (2014).

<sup>13</sup> B. Vermeersch and A. Shakouri, “Nonlocality in microscale heat conduction,” *ArXiv e-prints* (2014), arXiv:1412.6555v2.

<sup>14</sup> B. Vermeersch, J. Carrete, N. Mingo, and A. Shakouri, “Superdiffusive heat conduction in semiconductor alloys. I. Theoretical foundations,” *Phys. Rev. B* **91**, 085202 (2015).

<sup>15</sup> Chengyun Hua and A. J. Minnich, “Semi-analytical solution to the frequency-dependent Boltzmann transport equation for cross-plane heat conduction in thin films,” *J. Appl. Phys.* **117**, 175306 (2015).

<sup>16</sup> E. Abrahams, P. W. Anderson, D. C. Licciardello, and T. V. Ramakrishnan, “Scaling theory of localization: Ab-  
sence of quantum diffusion in two dimensions,” *Phys. Rev. Lett.* **42**, 673–676 (1979).

<sup>17</sup> Ping Sheng, *Introduction to Wave Scattering, Localization and Mesoscopic Phenomena*, 2<sup>nd</sup> edition (Springer, Berlin, 2005).

<sup>18</sup> T. R. Kirkpatrick, “Localization of acoustic waves,” *Phys. Rev. B* **31**, 5746–5755 (1985).

<sup>19</sup> M. N. Luckyanova, J. Mendoza, H. Lu, B. Song, S. Huang, J. Zhou, M. Li, Y. Dong, H. Zhou, J. Garlow, L. Wu, B. J. Kirby, A. J. Grutter, A. A. Puretzky, Y. Zhu, M. S. Dresselhaus, A. Gossard, and G. Chen, “Phonon localization in heat conduction,” *Science Advances* **4**, eaat9460 (2018).

<sup>20</sup> P. G. Klemens, “The scattering of low-frequency lattice waves by static imperfections,” *Proc. Phys. Soc. A* **68**, 1113–1128 (1955).

<sup>21</sup> G. D. Mahan, “Effect of atomic isotopes on phonon modes,” *Phys. Rev. B* **100**, 024307 (2019).